Hindawi
Advances in Mathematical Physics
Volume 2022, Article ID 2881207, 9 pages
https://doi.org/10.1155/2022/2881207

Research Article

A Fractional-Order Discrete Lorenz Map

Yanyun Xie

School of General Education, Chongqing Water Resources and Electric Engineering College, Chongqing 40216, China

Correspondence should be addressed to Yanyun Xie; xieyanyun2022@126.com

Received 1 July 2022; Revised 25 August 2022; Accepted 6 September 2022; Published 20 September 2022

Academic Editor: Qura tul Ain

In this paper, a discrete Lorenz map with the fractional difference is analyzed. Bifurcations of the map in commensurate-order and incommensurate-order cases are studied when an order and a parameter are varied. Hopf bifurcation and periodic-doubling cascade are found by the numerical simulations. The parameter values of Hopf bifurcation points are determined when the order is taken as a different value. It can be concluded that the parameter decreases as the order increases. Chaos control and synchronization for the fractional-order discrete Lorenz map are studied through designing the suitable controllers. The effectiveness of the controllers is illustrated by numerical simulations.

1. Introduction

Fractional calculus has been studied for a fairly long time in the field of pure mathematics [1]. At the primary stage, its development is slow because of the absence of geometrical interpretation and applications. Until the last few decades, researchers gradually noticed that fractional calculus has superior characteristics over the classical calculus. Nowadays, fractional calculus has been analyzed deeply in theoretical research and practical applications.

It is well known that discrete fractional calculus was put forward by Diaz and Olser [2]. Within the past decade, people are more and more interested in discrete fractional calculus. In [3–7], definitions and stability for discrete fractional calculus are introduced and investigated. Based on these, many fractional-order maps are proposed and studied in detail, such as fractional sine map, standard map, Hénon map, and Ikeda map [8–14]. For the long-term memory characteristic of the operator, this kind of maps is a better fit for application in secure communications and encryption [15–17]. The main reasons are that fractional-order discrete maps are not only sensitive to the small disturbance of parameters and initial conditions but also to the variation of fractional orders, which are the unique advantages of fractional-order systems. On the other hand, fractional-order discrete maps have simple forms and rich dynamics, which are good for model analysis and numerical computation. Therefore, investigation of a fractional-order discrete map including dynamics, stabilization, and synchronization is necessary and important for the development of fractional calculus.

In this paper, we will investigate a fractional-order discrete Lorenz map. Bifurcations of the map in commensurate-order and incommensurate-order cases are analyzed. Hopf bifurcation and periodic-doubling cascade are found by the numerical simulations. The parameter values of Hopf bifurcation points are determined when the order is varied. The fractional-order discrete Lorenz map has several advantages such as unpredictability, diffusion properties, sensitivity to initial conditions, orders, and parameters. It is very suitable for application in secure communication and encryption. Therefore, chaos control and synchronization for the fractional-order Lorenz map are studied through designing the suitable controllers based on the adaptive method. The advantages of the method are follows: the principle of the adaptive method is simple based on the stability theory of fractional difference maps; the designing controllers for control and synchronization are easy to realize in simulations. It should be noted that the research of fractional-order maps is at an early stage. Many control and synchronization methods and strategies need to be studied further.

The paper is organized into seven sections. Section 2 gives the related theories of discrete fractional calculus. A

fractional-order discrete Lorenz map is described in Section 3. Bifurcations in two cases are studied in Section 4. Control and synchronization for map are investigated, respectively, in Sections 5 and 6. The summarization of the paper is given in Section 7.

2. Discrete Fractional Calculus

In this section, some theories related to discrete fractional calculus will be listed. The symbol ${}^{C}\Delta_b^q Y(t)$ represents the Caputo type fractional difference of a function $Y(\mathrm{t})$: $\mathrm{N}_b \longrightarrow \mathbb{R}$ with $\mathrm{N}_b = \{b, b+1, b+2, \cdots\}$ [18], which is marked as

$$ {}^{C}\Delta_b^q Y(t) = \Delta_b^{-(n-q)} \Delta_b^n Y(t) = \frac{1}{\Gamma(n-q)} \sum_{s=b}^{t-(n-q)} (t-s-1)^{(n-q-1)} \Delta_s^n Y(s). \tag{1} $$

Here, $q \notin N$ is the fractional order, and $n = \lceil q \rceil + 1$.The fractional sum in (1) can be expressed as [19, 20]

$$ \Delta_b^{-q} Y(t) = \frac{1}{\Gamma(q)} \sum_{s=b}^{t-q} (t-s-1)^{(q-1)} Y(s). \tag{2} $$

Here, $t \in N_{b+q}$, $q > 0$, and the falling function $t^{(q)}$ is written as follows:

$$ t^{(q)} = \frac{\Gamma(t+1)}{\Gamma(t+1-q)}, \tag{3} $$

where $\Gamma(\cdot)$ denotes the gamma function, which is defined as $\Gamma(t) = \int_0^{+\infty} x^{t-1} e^{-x} dx$ for $t > 0$.

We can determine the numerical solutions of a fractional difference equation via the method below. A fractional difference equation with initial conditions is

$$ \begin{cases} {}^{C}\Delta_b^q u(t) = f(t+q-1, u(t+q-1)), \\ \Delta^k u(b) = u_k . n = \lceil q \rceil + 1, k = 0, 1, 2, \cdots, n-1. \end{cases} \tag{4} $$

The corresponding discrete integral equation is

$$ u(t) = u_0(t) + \frac{1}{\Gamma(q)} \sum_{s=b+n-q}^{t-q} (t-s-1)^{(q-1)} f(s+q-1, u(s+q-1)), t \in \mathrm{N}_{b+n}. \tag{5} $$

Here, $u_0(t) = \sum_{k=0}^{n-1} ((t-b)^{(k)} / \Gamma(k+1)) \Delta^k u(b)$.

The below theorem can be used to determine the stability of the equilibrium point for a fractional-order difference system. You can refer to the literature [21] for the detail of the proof.

Theorem 1. *For a linear fractional-order difference discrete system,*

$$ {}^{C}\Delta_b^q X(t) = \mathbf{A} Y(t+q-1). \tag{6} $$

Here, $Y(t) = (y_1(t), y_2(t), \cdots, y_n(t))^T$, $0 < q < 1$, $\mathbf{A} \in R^{n \times n}$ *and* $\forall t \in N_{b+1-q}$, *and the zero equilibrium is asymptotically stable if all the eigenvalues of matrix* $\mathbf{A}$ *satisfy*

$$ |\lambda_i| < \left(2 \cos \frac{|\arg \lambda_i| - \pi}{2 - q} \right)^q \text{ and } |\arg \lambda_i| > \frac{q\pi}{2}, i = 1, 2, \cdots, n. \tag{7} $$

Definition 2. For a fractional-order system, which can be described by ${}^{C}\Delta_a^q = f(\mathbf{x}(\mathrm{t}))$, where $\mathbf{x} = (x_1, x_2, \cdots, x_n)^{\mathrm{T}}$ is the state vector, $\mathbf{q} = (q_1, q_2, \cdots, q_n)^{\mathrm{T}}$ is the fractional derivative orders vector, and $q_i > 0$. The fractional-order system is in commensurate order when all the derivative orders satisfy $q_1 = q_2 = \cdots = q_n$; otherwise, it is an incommensurate-order system [22].

3. A Discrete Lorenz Map with Fractional Difference Operator

Recently, a Lorenz map was studied deeply and successfully applied in encryption [23–25]. A Lorenz chaotic map was presented which is given as follows:

$$ \begin{cases} x(n+1) = (1 + \gamma\delta) x(n) - \delta y(n) x(n), \\ y(n+1) = (1 - \delta) y(n) + \delta x^2(n). \end{cases} \tag{8} $$

Here, $x(n)$ and $y(n)$ denote state variables, and γ and δ represent system parameters. The corresponding first-order difference for (8) is expressed as

$$ \begin{cases} \Delta x(n) = x(n+1) - x(n) = (1 + \gamma\delta) x(n) - \delta y(n) x(n) - x(n), \\ \Delta y(n) = y(n+1) - y(n) = (1 - \delta) y(n) + \delta x^2(n) - y(n). \end{cases} \tag{9} $$

By using the Caputo-like delta difference operator to replace the first order difference in (9) with a starting point b, the fractional-order Lorenz map can be obtained, which is the following form [26]:

$$ \begin{cases} {}^{C}\Delta_b^q x(t) = (1 + \gamma\delta) x(t-1+q) - \delta y(t-1+q) x(t-1+q) - x(t-1+q), \\ {}^{C}\Delta_b^q y(t) = (1 - \delta) y(t-1+q) + \delta x^2(t-1+q) - y(t-1+q). \end{cases} \tag{10} $$

Here, $0 < q < 1$ denotes the derivative order. If all the orders in (10) are identical, then the map is a commensurate-order one. Otherwise, it is an incommensurate-order one which is expressed by the following difference equations:

$$ \begin{cases} {}^{C}\Delta_b^{q_1} x(t) = (1 + \gamma\delta) x(t-1+q_1) - \delta y(t-1+q_1) x(t-1+q_1) - x(t-1+q_1), \\ {}^{C}\Delta_b^{q_2} y(t) = (1 - \delta) y(t-1+q_2) + \delta x^2(t-1+q_2) - y(t-1+q_2). \end{cases} \tag{11} $$

The derivative orders satisfy $0 < q_1, q_2 < 1$.

The numerical formulas of commensurate-order map (10) are

$$\begin{cases} x(n) = x(b) + \dfrac{1}{\Gamma(q)} \displaystyle\sum_{j=1}^{n} \dfrac{\Gamma(n-j+q)}{\Gamma(n-j+1)} (\gamma\delta x(j-1) - \delta y(j-1)x(j-1)), \\ y(n) = y(b) + \dfrac{1}{\Gamma(q)} \displaystyle\sum_{j=1}^{n} \dfrac{\Gamma(n-j+q)}{\Gamma(n-j+1)} \left(\delta\left(-y(j-1) + x^2(j-1)\right)\right), \end{cases} \tag{12}$$

and the numerical recipes of (11) are as follows:

$$\begin{cases} x(n) = x(b) + \dfrac{1}{\Gamma(q_1)} \displaystyle\sum_{j=1}^{n} \dfrac{\Gamma(n-j+q_1)}{\Gamma(n-j+1)} (\gamma\delta x(j-1) - \delta y(j-1)x(j-1)), \\ y(n) = y(b) + \dfrac{1}{\Gamma(q_2)} \displaystyle\sum_{j=1}^{n} \dfrac{\Gamma(n-j+q_2)}{\Gamma(n-j+1)} \left(\delta\left(-y(j-1) + x^2(j-1)\right)\right). \end{cases} \tag{13}$$

In here, we fix the low limit b as 0. When the parameters are taken as $\gamma = 1.25, \delta = 0.75$, and the order q is 0.99, the commensurate-order map (10) has a chaotic attractor, see Figure 1.

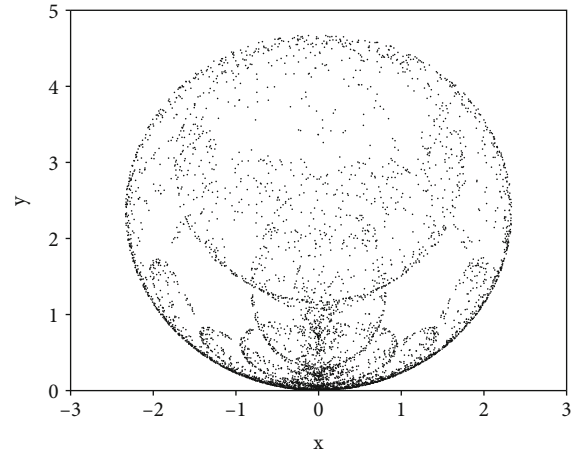

Figure 1: The chaotic attractor of map (10).

4. Bifurcations of Fractional-Order Discrete Lorenz Map

We will study the bifurcations of the fractional-order discrete Lorenz map in commensurate-order and incommensurate-order cases in this section.

4.1. Bifurcations of Map (10). Firstly, parameter γ is fixed as 1.25, and the intervals of δ and the order q are taken as $[0.2, 1]$ and $[0.6, 0.99]$, respectively. The bifurcation of the commensurate-order discrete Lorenz map, which is corresponding to the difference equations (10), is studied when δ and q are varied, see Figure 2(a), from which it is clear that that map (10) has very abundant dynamics. Period-doubling cascades and Hopf bifurcations can be observed. The chaos region becomes large as the order increases from 0.65 to 0.99. In order to obtain the order of chaos appears firstly in the map (10), a bifurcation diagram with the variation of the order in the interval $[0.6, 0.65]$ and parameter δ is plotted in Figure 2(b). It is clear that the map (10) is periodic when $q < 0.62$ and is chaotic when $q \geq 0.62$. Based on this, we can get the total order for the map (10) to remain chaos that is 1.24. The phase diagrams of map (10) with initial conditions $(x_0, y_0) = (0.1, 0)$ and $(x_0, y_0) = (-0.1, 0)$ belonging to different basins of attraction are plotted in Figure 3, in which the parameter δ increases from 0.30 to 0.60, and the order is taken as 0.95. Typical Hopf bifurcation can be observed from Figures 3(a) and 3(b). The two limit cycles become large as δ increases (Figure 3(c)). When $\delta = 0.60$, the two attractors merge into a chaotic one, see Figure 3(d).

Secondly, the parameter δ is chosen as 0.75, and the intervals of γ and the order are $[0.2, 1.3]$ and $[0.7, 0.99]$, respectively. Bifurcation of the map (10) when the parameter γ and the order q are varied is displayed in Figure 4(a). The region of chaos becomes large as the order increases from 0.65 to 0.99. A bifurcation diagram with the variation of the order in the interval $[0.70, 0.75]$ and parameter γ is plotted in Figure 4(b) to show the appearance of chaos in the map at the first time. It is clear that the map (10) is periodic when $q < 0.74$ and is chaotic when $q \geq 0.74$. Therefore, the total order of the map (10) to remain chaos is 1.48 in this case.

From Figures 2 and 4, we can see clearly that the route leading to chaos for map (10) is Hopf bifurcation. The Hopf bifurcation points (HPFs for short) for different values of the order q are listed in Table 1. It is clear that HPFs decrease as the order increases. An example is taken to show the Hopf bifurcation when the order $q = 0.95$. Map (10) converges to a fixed point for $\delta = 0.46$ (Figure 5(a)) and to a limit cycle for $\delta = 0.47$ (Figure 5(b)).

4.2. Bifurcations of Map (11). In this subsection, bifurcations of the incommensurate-order discrete Lorenz map which is corresponding to the difference equations (11) will be studied. Parameter γ is fixed as 1.25 and order $q_2 = 1$, and the interval of δ is $[0.2, 1]$. Figure 6(a) is the bifurcations of map (11) when δ and q_1 are varied. We can see that period-doubling and Hopf bifurcations occur when the parameter and the order are varied. The chaos region becomes large as the order increases from 0.4 to 0.99. From Figure 6(b), we can see that map (11) is periodic for $q_1 < 0.45$ and chaotic for $q_1 \geq 0.45$. Then, the total order for map (11) to remain chaos is 1.45 in this case.

Secondly, the order q_1 is fixed as 1, and the interval of q_2 is taken as $[0.35, 0.99]$. The bifurcations with the variation of the parameter δ and the order q_2 are shown in Figure 7. It can be seen that that the region of chaos becomes large as the order increases from 0.35 to 0.99. We can determine that the total order for map (11) to remain chaos is 1.4 based on Figure 7(b).

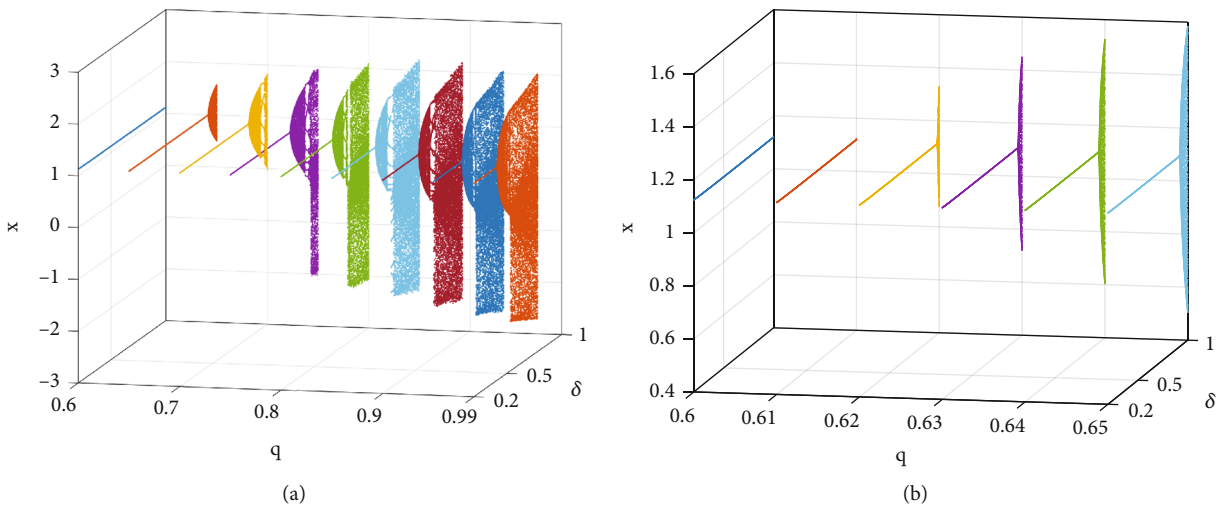

Figure 2: The bifurcation diagrams of map (10) when δ and q are varied. (a) $q \in [0.6, 0.99]$. (b) $q \in [0.6, 0.65]$.

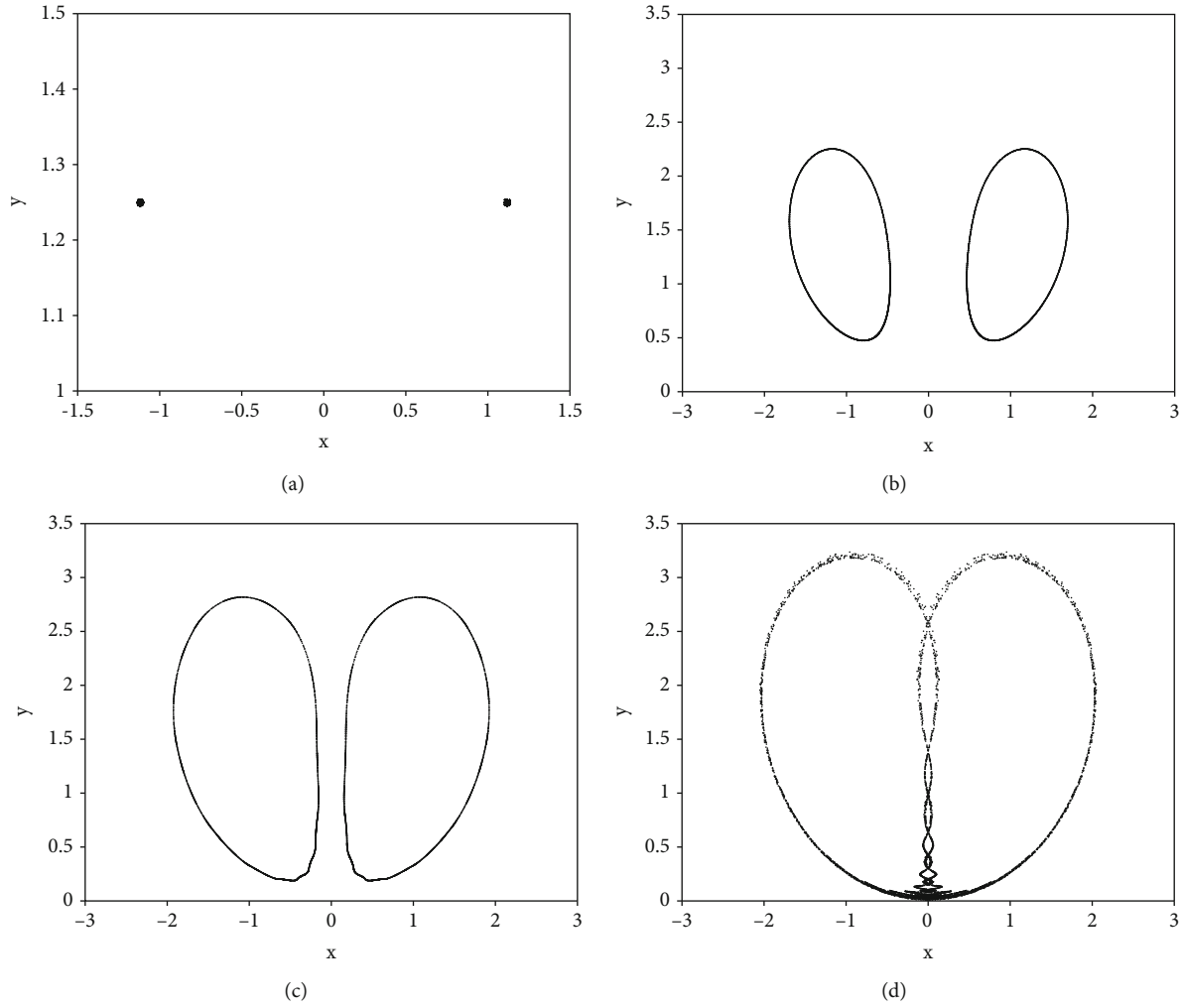

Figure 3: Phase diagrams of map (10) with different initial conditions $(x_0, y_0) = (0.1, 0)$ and $(x_0, y_0) = (-0.1, 0)$. (a) $\delta = 0.30$. (b) $\delta = 0.50$. (c) $\delta = 0.55$. (d) $\delta = 0.60$.

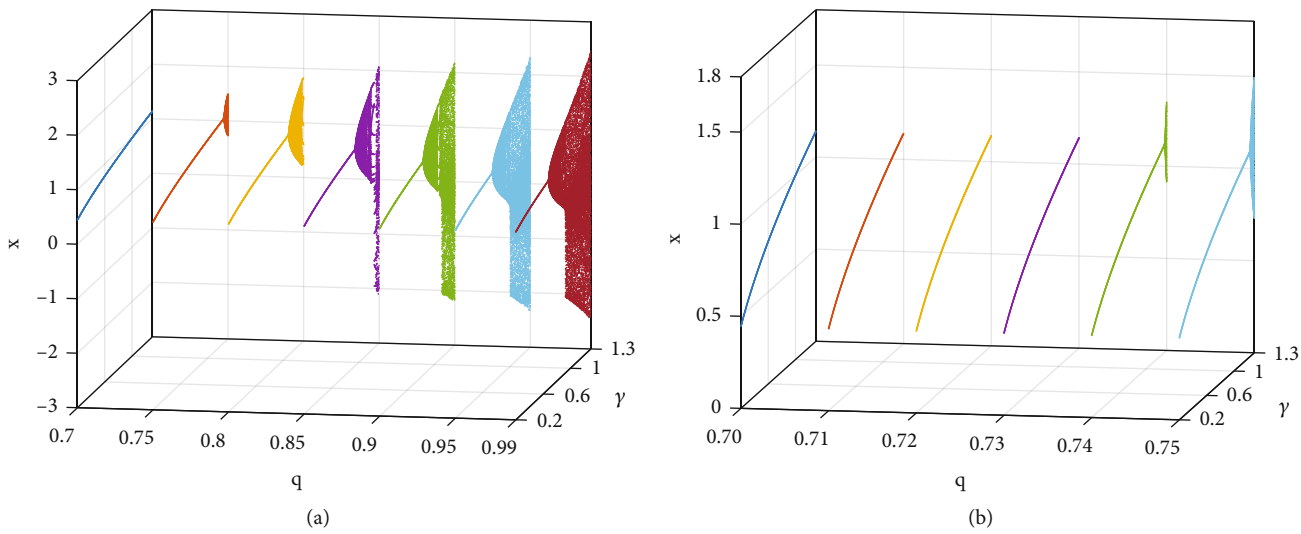

Figure 4: Bifurcation diagrams of map (10) when γ and q are varied. (a) $q \in [0.7, 0.99]$. (b) $q \in [0.7, 0.75]$.

Table 1: Hopf bifurcation points of map (10) for different values of q.

q	δ	q	δ
0.60	—	0.75	0.75
0.61	—	0.80	0.68
0.62	0.98	0.85	0.60
0.63	0.97	0.90	0.54
0.64	0.95	0.95	0.47
0.65	0.93	0.99	0.42
0.70	0.84		

5. Chaos Control

In this section, chaos control for map (10) will be analyzed. Firstly, map (10) with controllers is the follows:

$$\begin{cases} {}^{C}\Delta_b^q x(t) = (1+\gamma\delta)x(t-1+q) - \delta y(t-1+q)x(t-1+q) - x(t-1+q) + u_1(t-1+q), \\ {}^{C}\Delta_b^q y(t) = (1-\delta)y(t-1+q) + \delta x^2(t-1+q) - y(t-1+q) + u_2(t-1+q), \end{cases} \tag{14}$$

where u_1 and u_2 denote the chaos controllers.

Theorem 3. *If the controllers are taken as the following form,*

$$\begin{cases} u_1(t-1+q) = -(1+\gamma\delta)x(t-1+q) + \delta y(t-1+q)x(t-1+q)), \\ u_2(t-1+q) = -(1-\delta)y(t-1+q) - \delta x^2(t-1+q), \end{cases} \tag{15}$$

then the chaotic behavior of map (10) can be controlled.

Proof. By substituting (15) into (14), then map (14) can be rewritten as

$$\begin{cases} {}^{C}\Delta_b^q x(t) = -x(t-1+q), \\ {}^{C}\Delta_b^q y(t) = -y(t-1+q). \end{cases} \tag{16}$$

The compact form of map (16) is

$${}^{C}\Delta_b^q (x(t), y(t))^{\mathrm{T}} = \mathbf{B} \times (x(t-1+q), y(t-1+q))^{\mathrm{T}}, \tag{17}$$

where $\mathbf{B} = \begin{pmatrix} -1 & 0 \\ 0 & -1 \end{pmatrix}$. The eigenvalues of $\mathbf{B}$ satisfy $|\arg \lambda_i| = \pi$ and $|\lambda_i| = 2^q$, for $i = 1, 2$. It means that the chaotic behavior of map (10) can be controlled to the zero equilibrium based on Theorem 1.

The system parameters are fixed as $\gamma = 1.25$, $\delta = 0.75$ and order $q = 0.99$. Map (10) is stabilized by using the controllers when the iteration $n = 1000$, see Figure 8. We can see clear that $x(n), y(n)$ converge to zero as time n toward to 2000. □

6. Adaptive Synchronization

In here, adaptive synchronization for the Lorenz map in fractional form will be studied. Firstly, map (10) is chosen as the drive system and is rewritten as follows

$$\begin{cases} {}^{C}\Delta_b^q x_1(t) = \gamma\delta x_1(t-1+q) - \delta y_1(t-1+q)x_1(t-1+q), \\ {}^{C}\Delta_b^q y_1(t) = \delta\left(-y_1(t-1+q) + {x_1}^2(t-1+q)\right). \end{cases} \tag{18}$$

The response system with synchronization controllers $u_x(t-1+q)$ and $u_y(t-1+q)$ is designed as the following

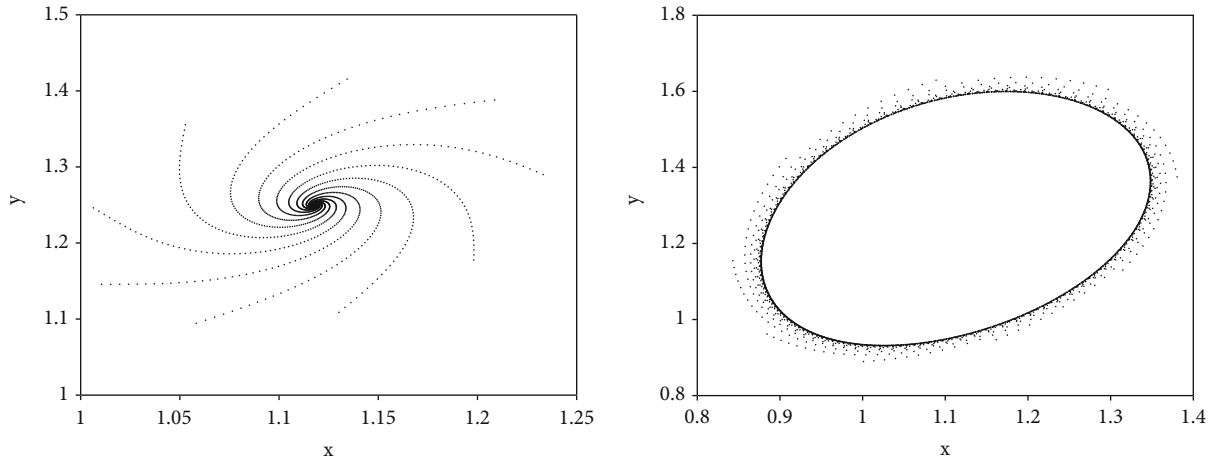

Figure 5: Phase diagrams of map (10) for $q = 0.95$. (a) $\delta = 0.46$. (b) $\delta = 0.47$.

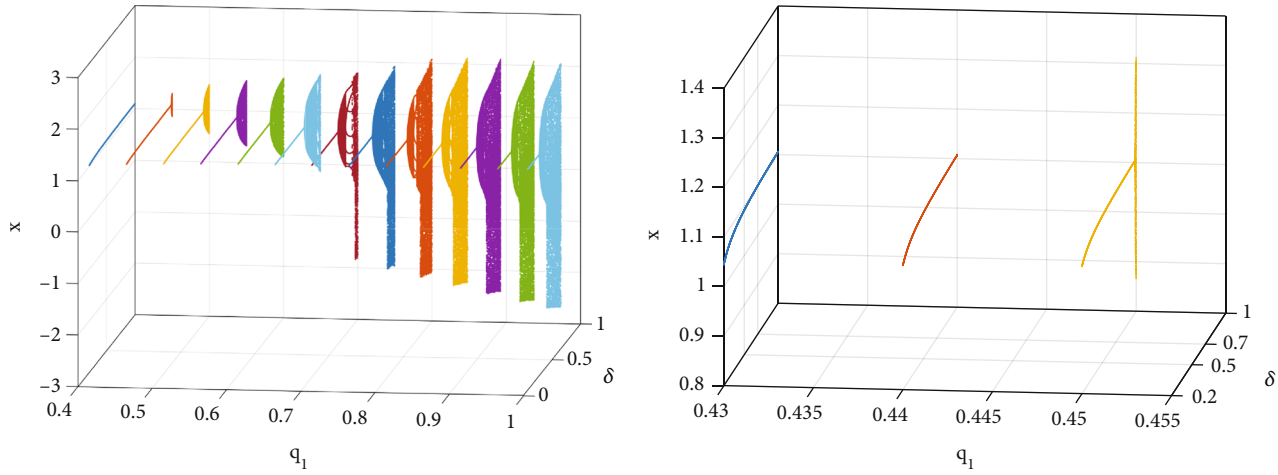

Figure 6: The bifurcation diagrams of map (11) when δ and q_1 are varied. (a) $q_1 \in [0.4, 0.99]$. (b) $q_1 \in [0.43, 0.45]$.

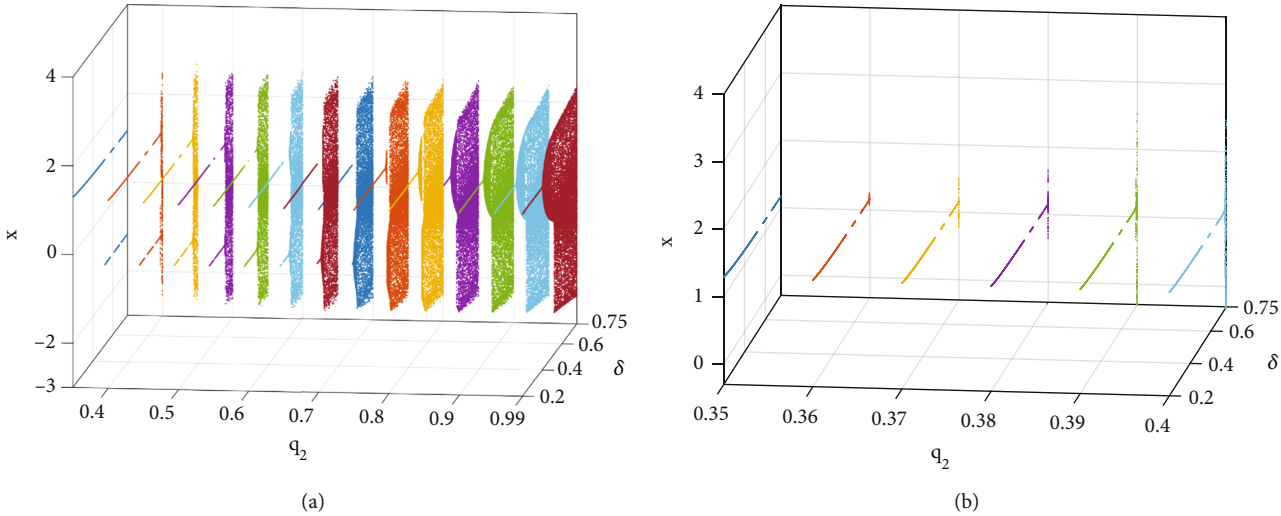

Figure 7: The bifurcation diagrams of map (11) when δ and q_2 are varied. (a) $q_2 \in [0.35, 0.99]$. (b) $q_2 \in [0.35, 0.4]$.

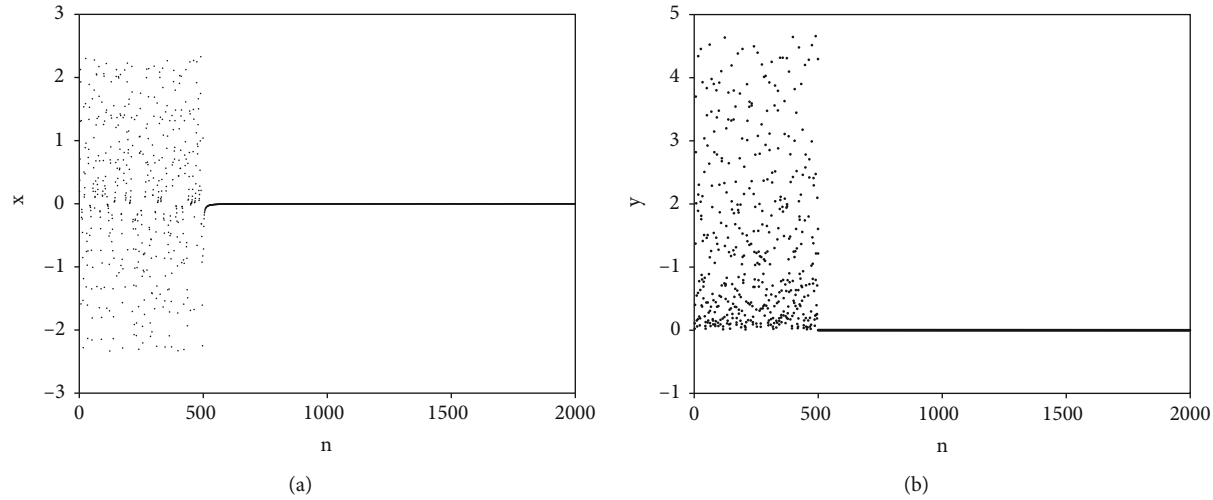

Figure 8: The controlled results for map (10). (a) The state variable x with n (b) the state variable y with n.

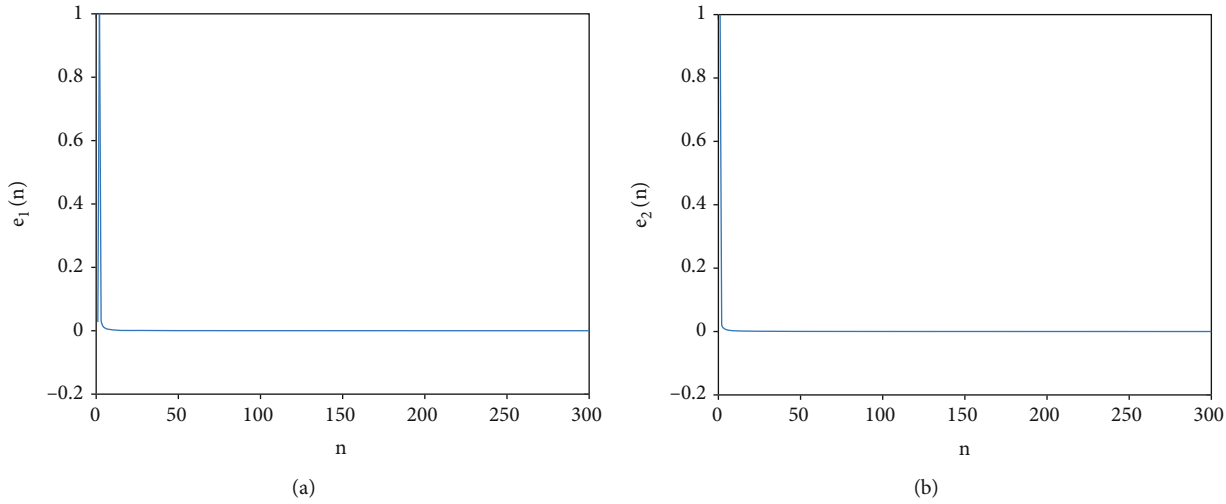

Figure 9: The synchronization results. (a) $e_1(n)$ with n. (b) $e_2(n)$ with n.

form:

$$\begin{cases} {}^{C}\Delta_b^{v} x_2(t) = \gamma\delta x_2(t-1+q) - \delta y_2(t-1+q)x_2(t-1+q) + u_x(t-1+q), \\ {}^{C}\Delta_b^{v} y_2(t) = \delta\left(-y_2(t-1+q) + {x_2}^2(t-1+q)\right) + u_y(t-1+q). \end{cases} \tag{19}$$

The error state variables of the synchronization are defined as

$$\begin{cases} e_1(t-1+q) = x_2(t-1+q) - x_1(t-1+q), \\ e_2(t-1+q) = y_2(t-1+q) - y_1(t-1+q). \end{cases} \tag{20}$$

It is well known that if the two error states variables converge to 0 as the time t tends to infinity, then maps (18) and (19) is synchronized under the controllers.

Theorem 4. *The synchronization between two maps (18) and (19) is realized if the controllers are designed as follows:*

$$\begin{cases} u_x(t-1+q) = (\delta y_2(t-1+q) - \gamma\delta - 1)e_1(t-1+q) + \delta x_1(t-1+q)e_2(t-1+q), \\ u_y(t-1+q) = (\delta - 1)e_2(t-1+q) - \delta(x_2(t-1+q) + x_1(t-1+q))e_1(t-1+q). \end{cases} \tag{21}$$

Proof. We can obtain the error system via simple computation

$$\begin{cases} {}^{C}\Delta_b^q e_1(t) = \gamma\delta x_2(t-1+q) - \delta y_2(t-1+q)x_2(t-1+q) - \gamma\delta x_1(t-1+q) + \delta y_1(t-1+q)x_1(t-1+q) + u_x(t-1+q), \\ {}^{C}\Delta_b^q e_2(t) = \delta\left(-y_2(t-1+q) + {x_2}^2(t-1+q)\right) - \delta\left(-y_1(t-1+q) + {x_1}^2(t-1+q)\right) + u_y(t-1+q). \end{cases} \tag{22}$$

By substituting the controllers (21) into (22), error dynamical system can be determined as the following:

$$\begin{cases} {}^{C}\Delta_a^q e_1(t) = -e_1(t-1+q), \\ {}^{C}\Delta_a^q e_2(t) = -e_2(t-1+q). \end{cases} \tag{23}$$

For the convenience of analysis, we give the compact form of system (23)

$${}^{C}\Delta_a^q(e_1(t), e_2(t)) = \mathbf{C} \times (e_1(t-1+q), e_2(t-1+q))^{\mathrm{T}}, \tag{24}$$

where $\mathbf{C} = \begin{bmatrix} -1 & 0 \\ 0 & -1 \end{bmatrix}$. Matrix $\mathbf{C}$ satisfies the stability condition

$$|\lambda_i| < \left(2\cos\frac{|\arg\lambda_i| - \pi}{2-q}\right)^q \text{ and } |\arg\lambda_i| > \frac{q\pi}{2}, i = 1, 2. \tag{25}$$

Therefore, synchronization between maps (18) and (19) is realized based on Theorem 1. In other words, the equilibrium point of (23) is asymptotically stable. □

In here, parameters are fixed as $\gamma = 1.25, \delta = 0.75$ and order $q = 0.99$. The initial conditions of maps (18) and (19) are chosen as $(0.2, 0.1), (0.7, 0.3)$. The synchronization results are plotted in Figure 9, from which we can see that e_1 and e_2 converge to zero rapidly as n towards to 300.

7. Conclusions

A fractional-order discrete Lorenz map is analyzed in this paper. Bifurcations of the map in commensurate-order and incommensurate-order cases are studied. The bifurcation diagrams in a three-dimension space are shown when a derivative order and a parameter are varied. Hopf and periodic-doubling bifurcations can be observed. Based on the analysis, parameter values of Hopf bifurcation points are determined with different orders. We can conclude that the critical values of the parameter decreases as the order increases. It is very important for us to observe the dynamical evolution of the map with the variation of an order and a system parameter. It is worth mentioning that it is the first time to show the dynamics of the fractional-order Lorenz map in a three-dimension space, from which we can see that the order is a very important parameter which affects the dynamics of a fractional-order map. Therefore, the map with an order has more extensively parametric space and abundant dynamics. Meanwhile, it is very important for the application of the map in secure communications and encryption. Chaos control and synchronization for the fractional-order discrete Lorenz map are studied through designing the suitable controllers. The effectiveness of the controllers is illustrated by numerical simulations. From the results, we can also see that a high speed of stabilization and synchronization is obtained.

Data Availability

The data for the bifurcation diagrams used to support the findings of this study are included within the supplementary information file(s) (available here).

Conflicts of Interest

The author declares no conflicts of interest regarding this article.

Authors' Contributions

The author has accepted responsibility for the entire content of this submitted manuscript and approved submission.

References

[1] C. Goodrich and A. C. Peterson, *Discrete fractional calculus*, Springer, Berlin, 2015.

[2] J. B. Diaz and T. J. Olser, "Differences of fractional order," *Mathematics of Computation*, vol. 28, no. 125, pp. 185–202, 1974.

[3] H. G. Sun, Y. Zhang, D. Baleanu, W. Chen, and Y. Q. Chen, "A new collection of real world applications of fractional calculus in science and engineering," *Communications in Nonlinear Science and Numerical Simulation*, vol. 64, pp. 213–231, 2018.

[4] M. Buslowicz and A. Ruszewski, "Necessary and sufficient conditions for stability of fractional discrete-time linear state-space systems," *Bulletin of the Polish Academy of Sciences. Technical Sciences*, vol. 61, no. 4, pp. 779–786, 2013.

[5] F. M. Atici and P. W. Eloe, "Discrete fractional calculus with the Nabla operator," *Electronic Journal of Qualitative Theory of Differential Equations*, vol. 3, no. 3, pp. 1–12, 2009.

[6] C. Goodrich, "Some new existence results for fractional difference equations," *International Journal of Dynamical Systems and Differential equations*, vol. 3, no. 1-2, pp. 145–162, 2011.

[7] D. Baleanu, G. Wu, Y. Bai, and F. Chen, "Stability analysis of Caputo-like discrete fractional systems," *Communications in Nonlinear Science and Numerical Simulation*, vol. 48, pp. 520–530, 2017.

[8] J. Mumkhamar, "Chaos in a fractional order logistic map," *Fractional Calculus and Applied Analysis*, vol. 16, no. 3, pp. 511–519, 2013.

[9] G. C. Wu, D. Baleanu, and S. D. Zeng, "Discrete chaos in fractional sine and standard maps," *Physics Letters A*, vol. 378, no. 5-6, pp. 484–487, 2014.

[10] C. Ma, J. Mou, P. Li, and T. Liu, "Dynamic analysis of a new two-dimensional map in three forms: integer-order, fractional-order and improper fractional-order," *The European Physical Journal Special Topics*, vol. 230, no. 7-8, pp. 1945–1957, 2021.

[11] T. Hu, "Discrete chaos in fractional Hénon map," *Applications of Mathematics*, vol. 5, no. 15, pp. 2243–2248, 2014.

[12] Y. Liu, "Chaotic synchronization between linearly coupled discrete fractional Hénon maps," *Indian Journal of Physics*, vol. 90, no. 3, pp. 313–317, 2016.

[13] O. Megherbi, H. Hamiche, S. Djennoune, and M. Bettayeb, "A new contribution for the impulsive synchronization of fractional-order discrete–time chaotic systems," *Nonlinear Dynamics*, vol. 90, no. 3, pp. 1519–1533, 2017.

[14] A. Ouannas, A. A. Khennaoul, Z. Odibat, and V. T. Pham, "On the dynamics, control and synchronization of fractional-order Ikeda map," *Chaos Solitions Fractals*, vol. 123, pp. 108–115, 2019.

[15] Z. Y. Liu, T. C. Xia, and Y. P. Wang, "Image encryption technology based on fractional two-dimensional discrete chaotic map accompanied with menezes-vanstone elliptic curve cryptosystem," *Fractals*, vol. 29, no. 3, p. 2150064, 2021.

[16] G. C. Wu, D. Baleanu, and Z. X. Lin, "Image encryption technique based on fractional chaotic time series," *Journal of Vibration and Control*, vol. 22, no. 8, pp. 2092–2099, 2016.

[17] J. X. Liu, Z. X. Wang, M. L. Shu, F. F. Zhang, S. Leng, and X. H. Sun, "Secure communication of fractional complex chaotic systems based on fractional difference function synchronization," *Complexity*, vol. 2019, Article ID 7242791, 10 pages, 2019.

[18] T. Abdeljawad, "On Riemann and Caputo fractional differences," *Computers & Mathematcs with Applications*, vol. 62, no. 3, pp. 1602–1611, 2011.

[19] H. I. Gray and N. F. Zhang, "On a new definition of the fractional difference," *Mathematics of Computation*, vol. 50, no. 182, pp. 513–529, 1988.

[20] K. S. Miller and B. Ross, *Univalent Functions, Fractional Calculus, and their Applications*, Eills Howard, Chichester, 1989.

[21] J. Čermák, I. Györi, and L. Něchvátal, "On explicit stability conditions for a linear fractional difference system," *Fractional Calculus and Applied Analysis*, vol. 18, no. 3, pp. 651–672, 2015.

[22] M. T. Shatnawi, N. Djenina, A. Ouannas, I. M. Batiha, and G. Grassi, "Novel convenient conditions for the stability of nonlinear incommensurate fractional-order difference systems," *Alexandria Engineering Journal*, vol. 61, no. 2, pp. 1655–1663, 2022.

[23] O. M. Al-Hazaimeh, M. F. Al-Jamal, N. Alhindawi, and A. Omari, "Image encryption algorithm based on Lorenz chaotic map with dynamic secret keys," *Neural Computing and Applications*, vol. 31, no. 7, pp. 2395–2405, 2019.

[24] O. M. Al-Hazaimeh, "A new dynamic speech encryption algorithm based on Lorenz chaotic map over internet protocol," *International Journal of Electrical and Computer Engineering*, vol. 10, no. 5, pp. 4824–8708, 2020.

[25] M. Itoh, T. Yang, and L. O. Chua, "Conditions for impulsive synchronization of chaotic and hyperchaotic SYSTEMS," *International Journal of Bifurcation and Chaos*, vol. 11, no. 2, pp. 551–560, 2001.

[26] A. A. Khennaoui, A. Ouannas, S. Bendoukha, G. Grassi, R. P. Lozi, and V. T. Pham, "On fractional-order discrete-time systems: Chaos, stabilization and synchronization," *Chaos Solitions Fractals*, vol. 119, pp. 150–162, 2019.